Radiation Measurements 155 (2022) 106789

Contents lists available at ScienceDirect

Radiation Measurements

journal homepage: www.elsevier.com/locate/radmeas

Anomalous fading in thermoluminescence signal of ten different K-feldspar samples and correlation to structural state characteristics

G.S. Polymeris [a,*], V. Giannoulatou [b], K.M. Paraskevopoulos [c], V. Pagonis [d], G. Kitis [b]

[a] Institute of Nanosciences and Nanotechnology, NCSR "Demokritos", Ag. Paraskevi, 15310, Athens, Greece
[b] Nuclear Physics Laboratory, Aristotle University of Thessaloniki, 54124, Thessaloniki, Greece
[c] Solid State Section, Physics Department, Aristotle University of Thessaloniki, 54124, Thessaloniki, Greece
[d] McDaniel College, Physics Department, Westminster, MD, 21157, USA

ARTICLE INFO

Keywords:
Thermoluminescence
Anomalous fading
Structural characteristics
K-feldspars

ABSTRACT

The present work reports an extended study of anomalous fading (AF) in the TL signal of ten different pure K-feldspar samples from North Greece. A fading protocol was applied, including a standard series of TL measurements undertaken following a variety of storage times after irradiation, in order to plot the luminescence output as a function of storage time. Anomalous fading was found to be ubiquitous for the TL signal of all feldspars. The remnant signals are defined as the ratio of the TL signal remaining after storage time t, over the corresponding signal promptly measured. Two different fading rates were calculated, namely the value of g-factor which describes the luminescence signal loss in terms of percentage per decade of time as well as the g_{50}-factor which describes the fading rate when the signal has been reduced to 50% of the prompt value measured after irradiation due to AF. Both aforementioned fading factors were calculated over the entire TL glow curves in step intervals of 10 °C and were eventually plotted versus glow curve temperature. The analysis indicated that fading factors yield maximum values within the temperature range between 200 and 350 °C, with a tendency to decrease with increasing temperature along the rest glow curve. As the 10 K-feldspar samples belong to three different groups (microclines, sanidines and orthoclases), possible correlation is studied between the fading factors and specific structural parameters of alkali feldspars, such as the probability of Al-cation to occupy specific sites in the forming tetrahedra and the volume of the unit cell.

1. Introduction

Athermal or anomalous fading (hereafter AF) of thermoluminescence (TL) signals is the term adopted for the rapid decay of luminescence, instead of the stability expected for it according to standard luminescence kinetic models (Wintle, 1973; Chen and McKeever, 1997). Previous works have been careful to differentiate between processes which can be accelerated by heating and those which operate independent of the temperature of storage (Sanderson, 1988; Spooner, 1994). It stands as experimental drawback against effectively using feldspars as a luminescence chronometer. In many cases, AF is also monitored for the case of either optically or infrared stimulated luminescence (OSL and IRSL, respectively). Despite the detrimental effect of AF to the final ages, there have been proposed various attempts to circumvent it. These attempts include (a) correcting the ages by calculation of an appropriate factor (Huntley and Lamothe, 2001); (b) adopting experimental protocols with two or multi steps of IRSL, where the second or the last measurement takes place at elevated temperature (Thomsen et al., 2008; Buylaert et al., 2009); (c) isolating the most stable signal using the appropriate mathematical models and deconvolution (Pagonis et al., 2021); and (d) measuring alternative luminescence signals, such as Thermally Assisted Optically Stimulated Luminescence (TA – OSL, Polymeris et al., 2015) and Infrared Photoluminescence (IRPL, Prasad et al., 2017).

During the last decade, a collection of various K-feldspar samples from igneous rocks of Northern Greece has stimulated basic research on the luminescence properties of K-feldspars as an attractive topic for our research group. These samples were repeatedly studied towards an effort to correlate luminescence features such as TL/OSL/IRSL intensity with structural state characteristics (Polymeris et al., 2013, 2017; Pagonis et al., 2015, 2020, 2021; Sfampa et al., 2015, 2019; Kitis et al., 2016; Şahiner et al., 2017; Angeli et al., 2020). All previous found good

* Corresponding author.
E-mail address: g.polymeris@inn.demokritos.gr (G.S. Polymeris).

https://doi.org/10.1016/j.radmeas.2022.106789
Received 23 November 2021; Received in revised form 10 May 2022; Accepted 14 May 2022
Available online 19 May 2022
1350-4487/

correlation between individual K-feldspar structure and various stimulated luminescence features, mostly for TL and IRSL signals. Besides intensities, bleaching and model dependent parameters that describe the IRSL phenomenon in feldspars were also correlated. It is critical to note that no previous study on AF has ever been reported so far in the literature for these specific museum samples of K-feldspars.

In contrast, AF in TL, OSL, IRSL and TA - OSL signals has been meticulously studied for the case of Durango apatite; a reference material as it yields extremely intense athermal fading effect. AF in Durango apatite was studied as a function of (a) grain size in both micrometer and nanometer ranges, (b) annealing temperature, (c) predose and irradiation temperature, (d) heating rate as well as (e) the occupancy of the recombination sites. For a review in the related literature, readers could refer to Polymeris et al. (2018 and references therein). In this latter study, AF was studied throughout the entire temperature range of the TL glow curve differentially, namely in intervals of 10 °C; through this aforementioned analysis of the AF, these authors have pointed out that the effect in nano-sized Durango apatite yields minor dependence on the TL glow curve temperature. The aim of the present study is twofold, including (a) an attempt to study AF within the entire temperature range of the TL signal of these museum samples of K-feldspars performing an analysis similar to that reported by Polymeris et al. (2018), along with (b) possible correlation of the effect to the structure of the samples.

2. Experimental

2.1. Materials

In very general terms, the basic structure of an alkali feldspar consists of a three dimensional array of corner-sharing AlO_4 and SiO_4 tetrahedra. Three out of the four T-cation sites are occupied by a Si-cation, and the fourth by an Al-cation. The structure of sanidines contains two distinct Si/Al tetrahedral sites, denoted by T_1 and T_2, being monoclinic. By contrast, microclines are the low temperature form and the corresponding unit cell is triclinic, with highly ordered distribution of Al/Si cations among four distinguishable tetrahedral sites, denoted by $T_1(o)$, $T_2(o)$, $T_1(m)$ and $T_2(m)$. Orthoclases used to be considered an intermediate form between sanidines and microclines. Nevertheless, while most microcline samples show fine-scale tartan twinning, the group including orthoclases is now known to have a complex "tweed" texture revealed by high resolution electron microscopy. The use of both FTIR and powder XRD analysis (Ribbe, 1983; Kroll and Ribbe, 1987; Theodosoglou et al., 2010; Polymeris et al., 2013) has enabled not only the identification of the samples, but also the calculation of basic structural state characteristics, such as the unit cell volume as well as the probability of the Al-cation to occupy the $T_1(o)$ and $T_1(m)$ sites $\Sigma t_1 = t_{1m} + t_{10}$. There is a straightforward, monotonic increase of both aforementioned parameters as one moves from sanidines to orthoclases and eventually to microclines.

The present study was conducted to a group consisting of ten naturally occurring pure K-feldspar samples from igneous rocks of Northern Greece; these are the same samples that have been previously studied by Polymeris et al. (2013, 2017), Pagonis et al. (2015, 2020, 2021), Sfampa et al. (2015, 2019), Kitis et al. (2016), Şahiner et al. (2017) and Angeli et al. (2020). Both handling and chemical pretreatments of these samples were previously described by Theodosoglou et al. (2010); thus these will not be repeated here. These K-feldspars include samples from all three groups, namely microclines, sanidines and orthoclases. Samples from these three groups are almost identical in their physical properties, and it is impossible to distinguish between them without either X-ray diffraction (XRD) or Fourier Transform Infrared (FTIR) spectroscopy analysis. The only difference is their crystal structure. Classification of the K-feldspar samples into orthoclase, microcline and sanidine is made by Theodosoglou et al. (2010) using both FTIR and XRD analysis and the identification of specific vibrational modes and diffraction peaks respectively. Fig. 1 presents the dependence of the unit cell volume of these samples on the probability Σt_1.

2.2. Apparatus

The TL measurements for these feldspar samples were carried out using a Risø TL/OSL reader (model TL/OSL-DA-20), equipped with $^{90}Sr/^{90}Y$ beta particle source, delivering a nominal dose rate of 0.105 Gy/s (Bøtter-Jensen et al., 2000). A 9635QA photomultiplier tube with a combination of Pilkington HA-3 heat absorbing and a Corning blue filter was used for light detection. All measurements were performed with low constant heating rates of 1 K/s in order to avoid significant temperature lag (Kitis et al., 2015), and the samples were heated up to the maximum temperature of 500 °C. The grain size of the samples was 90–150 μm. Aliquots with mass of 7.5 mg each, were prepared by mounting the material on stainless-steel disks of 1 cm^2 area. Prior TL measurements, all feldspar samples were annealed at 900 °C for 1 h.

2.3. Protocol

A typical protocol to study fading includes a standard series of TL measurements undertaken following a variety of storage times after irradiation, in order to plot the luminescence output as a function of storage or fading time (Visocekas et al., 1994; Duller, 1997; Polymeris et al., 2006, 2014). The protocol that was applied in the framework of the present study is the same as used in our previous related studies; its various steps are presented in Table 1.

3. Method of analysis

In the present study, the TL signals that were measured in the framework of the current AF experiment correspond to the signals remaining after various times which have elapsed since the end of irradiation. Taking measurements of the corresponding TL signal promptly after an irradiation in the laboratory is crucial. Nevertheless, during step 2, the exact zero storage time is not zero; there is always a minimum time elapsed between the end of the irradiation and the following TL measurement. In the case of the Risø TL/OSL Reader that was used, this time interval is configured to be 120s. A good approximation to the effective fading time is half of the irradiation time (according to Auclair et al., 2003) plus the delay between end of irradiation and start of the measurement for calculating the g-value. Thus, storage

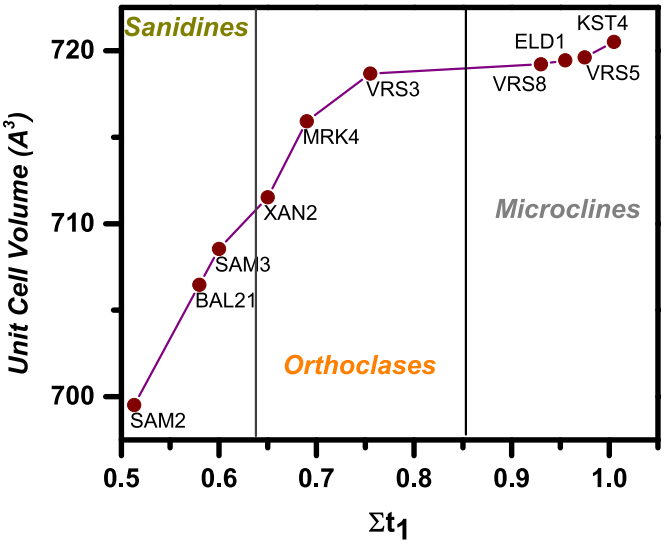

Fig. 1. The dependence of the unit cell volume on the probability of the Al-cation to occupy the T_1 sites $\Sigma t_1 = t_{1m} + t_{10}$.

Table 1
The protocol for the AF measurements of the present study.

Protocol's Steps	Protocol's Actions
1	Test Dose (50 Gy).
2	TL measurement to obtain the initial sensitivity TL_0.
3	Test Dose (50 Gy)
4	Storage in dark for duration $t_1 = 6$ h
5	Residual TL_1 (R-TL_1 hereafter) measurement
6	Repeat steps 3–5 for 12 different storage times t_i, ranging up to 2 months

time also includes part of the irradiation time. As test dose was 50 Gy, irradiation time was roughly 500s. Thus, 250s were added to the storage time. Consequently, all corresponding durations are added to the storage time sequence of step 2 (Aitken, 1985; Polymeris et al., 2018).

For each storage time, a background measurement was performed, namely measurement to look at the black body radiation, and during the analysis was subtracted from the corresponding measurement. Remnant TL signals are defined as the ratio of the TL signal remaining after storage time t, over the corresponding prompt TL signal measured after the end of the irradiation. The expression that finally describes the dependence of this aforementioned ratio is as follows (Aitken, 1985; Chen and McKeever, 1997; Polymeris et al., 2014):

$$\frac{TL_i}{TL_0} = 1 - \frac{g}{100} \cdot log_{10}\frac{t}{t_0}, \quad (1)$$

where TL_0 stands as the prompt measured luminescence signal at initial time, t_0 after the end of irradiation and TL_i the signal after storage time t_i. Eq. (1) gives directly the value of g-factor which describes the luminescence signal loss in terms of percentage per decade of time as a fitting parameter.

Besides the percentage TL signal loss per decade of time, the fading parameter g_{50} was also calculated. It represents the g-factor when the TL signal has been reduced to 50% of the prompt value measured after irradiation due to AF. The mathematical formulation of the g_{50}-factor was described by Pagonis and Kitis (2015), based on the model that was previously suggested by Jain et al. (2012). According to these two citations, the final expression that was used is the following (Polymeris et al., 2018):

$$\frac{TL_i}{TL_0} = \exp\left(- 12.167 \cdot \rho' \cdot \left[log_{10}(s \cdot t)^3 \right] \right) \quad (2)$$

where ρ' (cm^{-3}) is a dimensionless parameter denoting the density of recombination centers and s (s^{-1}) represents the frequency factor characterizing the tunneling process taking place from the ground state of the system (Pagonis et al., 2013; Pagonis and Kitis, 2015). However, regarding the parameters in Eq. (2), the analytical equation does not result in a direct calculation of the AF factor as in the case of Eq. (1). So, Pagonis and Kitis (2015); Kitis et al. (2015) attempted to correlate the dimensionless parameters ρ' of Eq. (2) with the g-factor of Eq. (1), by suggesting the following expression:

$$g_{50} = 2.7035 \cdot \rho'^{1/3} \quad (3)$$

In the framework of the present study, fading rate values will be evaluated via the calculation of g_{50} and g-factors. It is worth mentioning that all the expressions applied in the present work are derived assuming that the AF is attributed to quantum mechanical tunneling effect (Wintle, 1977; Jain et al., 2012). Both values of g_{50} and g-parameters were calculated for intervals of 10 °C throughout the entire TL glow curve region over all potassium feldspar samples by fitting the experimental data using Eq. (1) and by treating it as the unique fitting parameter; this analysis will be termed interval AF analysis. Special focus has been devoted to the temperature region where the naturally irradiated signal is measured, namely roughly between 200 and 400 °C. In each case, the goodness of fit was tested using the Figure Of Merit (F.O.M.) of Balian and Eddy (1977). For the direct fitting parameters (g and ρ'), the corresponding error for each value was calculated as the error in the fitting analysis; the corresponding F.O.M. value represents the error percentage. For each value of g_{50}, standard error propagation analysis was applied.

4. Results and discussion

AF stands as an effect that is present in all K-feldspar samples of the present study. Fig. 2a and b presents a group of residual TL glow curves for a microcline and a sanidine K-feldspar sample respectively, and selected storage times, with laboratory codes KST4 (microcline) and SAM2 (sanidine). It is quite interesting to note that, despite the fact that all TL glow curves where measured up to 500 °C, measurable and intense signal is measured up to almost 400–450 °C (test dose 50 Gy, heating rate 1 K/s). These two examples of glow curves are presented as typical for all other samples, since the behavior is identical in terms of both glow curve shapes and fading behavior. According to both Fig. 2a and b as well as to Polymeris et al. (2013), some among these samples yield a TL peak at temperatures lower than 100 °C (heating rate 1 K/s), corresponding to one shallow trap; the signal loss monitored for this specific TL peak is clearly seen due to the lifetime of the specific charge at room temperature. However, this peak is neither always prominent due to overlapping with the rest TL signal, nor interesting in the present study, as it yields thermal fading. At this point it is quite important to note that the TL glow curves of all K-feldspar samples do not yield other prominent TL glow peaks, besides this aforementioned shallow one. Nevertheless, signal loss takes place throughout the temperature range of the quite complex TL glow curves, namely within the temperature region between 150 and 450 °C, where a continuum of TL intensities is yielded. Within this region, fading gets contributions from both thermal and anomalous signal loss. For this reason, the analysis that was suggested for the present study will help in identifying the temperature range at which the signal loss is seen simply due to the lifetime of charge at room temperature. As the expressions applied in the present work are derived assuming that the AF is attributed to quantum mechanical tunneling effect, when athermal or anomalous fading becomes dominant, g and g_{50} values are expected to yield stable values within errors.

The effect of AF is quite fast for initial short storage times, while as this fading time gets more prolonged, fading rate decreases rapidly. As Fig. 2 reveal, fading does not influence all electron traps responsible for the TL signal in the same manner. AF is much stronger in the low temperature part of the TL glow curve, where both thermal and athermal fading take place, while the effect of fading decreases gradually as the temperature increases along the TL glow-curve. Moreover, in all K-feldspars there is a part of the high-temperature TL glow curve which remains unaffected; for temperatures over 400 °C the TL glow curves of all storage times coincide. In other words, there is a significant part of the TL signal that is left unfaded. This behavior is characteristic of a localized transition and has been reported recently by Pagonis et al. (2013, 2014). It is the well known wave-front behavior, as it was named by Sfampa et al. (2015) in their bleaching experiments using IRSL. The temperature range of this unaffected part of the TL glow curve increases for the orthoclase group of K-feldspars, while for the other two groups it remains about the same. Similar features were also reported by Sfampa et al. (2015) for the part of the high-temperature TL glow curve which remains unaffected by the IRSL bleaching, no matter how long the stimulation time be. The corresponding fading behavior in apatites was slightly different, as AF occurs throughout the temperature range within RT and 500 °C (Polymeris et al., 2014).

Fig. 2c and d present the corresponding results of the interval AF analysis on the AF of the same two K-feldspar samples. This analysis consists of calculating both g and g_{50} fading factors within intervals over 10 °C within the entire TL glow curve and plotting them versus TL glow curve temperature, covering the temperature region between 130 and

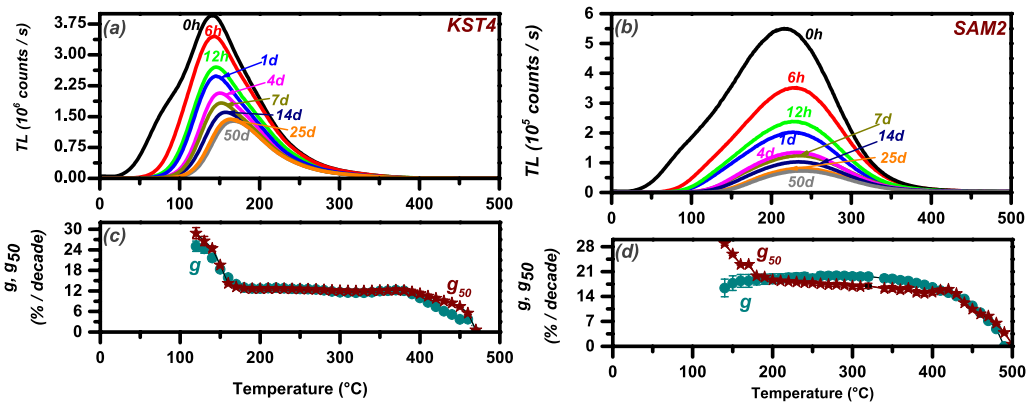

Fig. 2. Plots **a** and **b** present the TL glow curves that were measured following various storage times and subsequent TL measurement for two different K-feldspar samples, namely a sanidine (SAM2) and a microcline (KST4). Plots **c** and **d** present the corresponding *g* and g_{50} fading factors plotted versus TL glow curve temperature.

500 °C, for the reasons that were just previously described. It must be noticed that, according to this figure, the g_{50}-factor differs from the *g*-factor, since these two parameters were calculated using different models. However, as it is also demonstrated by Fig. 2a and b, in most cases the g_{50}-factor values and the *g*-factor values do not differ substantially. Fig. 3 presents, for the same fading data set (corresponding to representative temperature interval between 290 and 300 °C for the sample MRK4), examples of fitting using both equation (1) for calculating the *g* value (Fig. 3a) as well as equation (2) for the calculation of the g_{50} value (Fig. 3b). Experimentally obtained data are presented as dots while the best-fit as line. Fig. 3c and d present the fitting residuals of plots **3a** and **3b** respectively. Both models approximate the data well. As the residuals indicate, equation (1) indicates better results for longer fading times while the model of Pagonis and Kitis (2015) (equation (2)) approximates better the data at short storage times.

Another prominent feature of Fig. 2 deals with the values of either fading parameter throughout the entire TL glow curve region; none is stable over the temperature region of the present study. Such dependence of the fading rate on the TL glow curve temperature is both obvious as well as prevalent for temperatures over 400 °C, where the values of both factors decrease substantially; nevertheless it exists even for temperatures below 400 °C. This is another hint towards a temperature dependent behavior of the AF in K-feldspars samples as well, besides apatites (Polymeris et al., 2018). This thermal dependent behavior is also demonstrated by Fig. 4, presenting the dependence of the remnant TL after 30 days storage time (namely the ratio $\frac{TL_{30\ days}}{TL_0}$) over the entire TL glow curve temperature range. According to Bowman (1988) this ratio should give the anomalous fading factor as a function of the glow-curve temperature. According to these plots, AF rate presents wide

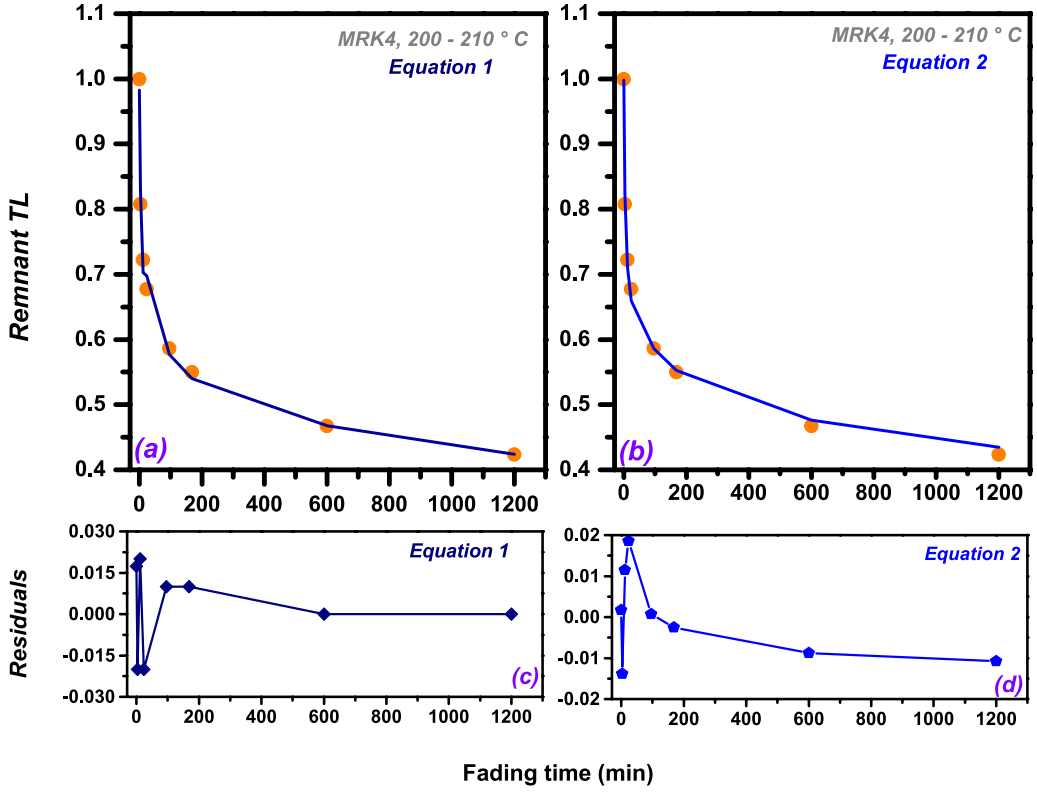

Fig. 3. Examples of remnant TL fitted using both models, namely equation (1) (plot **a**) and equation (2) (plot **b**). Plots **c** and **d** present the corresponding fitting residuals.

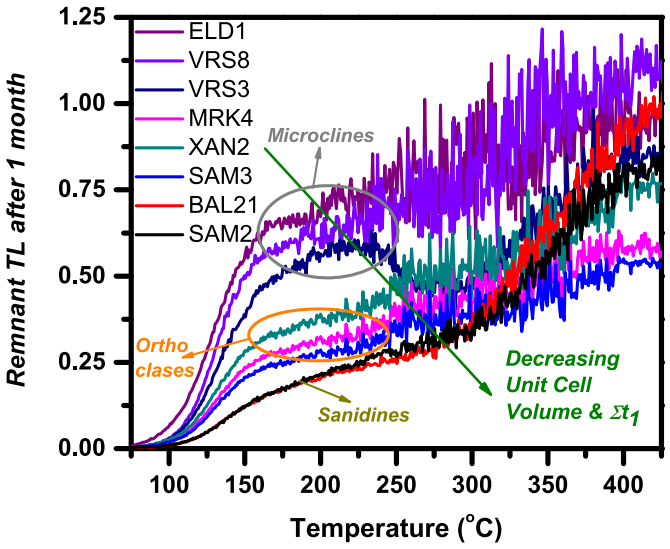

Fig. 4. Remnant TL following storage of 1 month, plotted versus the TL glow curve temperature.

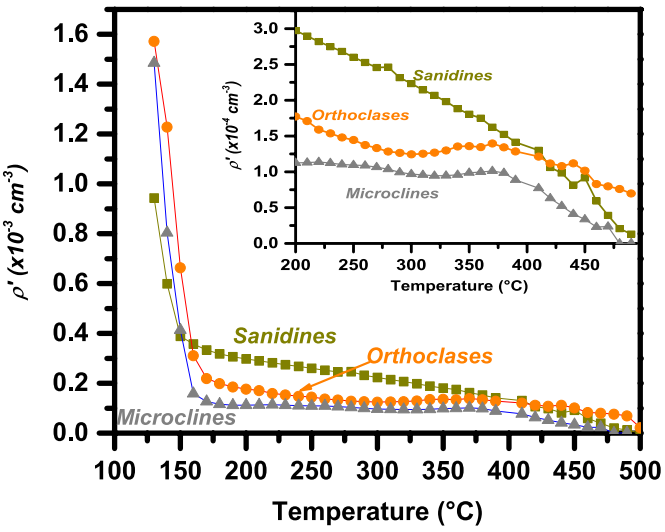

Fig. 6. The behavior of the parameter ρ' versus the TL glow curve temperature for a selection of samples that include one microcline, one sanidine and one orthoclase. Inset presents a detail of the main plot for TL glow curve temperatures beyond 200 °C.

plateau regions, located within the temperature part below 250 °C. Nevertheless, one can argue that these plateaus are slopping towards lower temperatures than being flat, showing a break in slope below 250 °C. In any case, the temperature range of this plateau strongly depends on the type of K-feldspar, being wider for the case of sanidines. Moreover, thermal dependence of AF rate is much different in apatites, where more than one plateau region could be easily identified within the temperature range up to 500 °C (Polymeris et al., 2014), while the last plateau that corresponds to deep traps with delocalization temperatures over 450 °C lying very close to the value of unity (Polymeris et al., 2014).

Nevertheless, the most interesting feature that Fig. 4 yields, deals with the dependence of the level of the remnant TL following storage for 1 month on the type of K-feldspars. Microclines indicate much more intense residual TL levels than the other two types of K-feldspars. At the same time, fading is more intense in sanidines, resulting in the lowest level of the signal acquired. The values of the remnant TL after 30 days show clear tendency to decrease with decreasing unit cell volume. Nevertheless, a clear discrimination among the remnant TL values of different groups is not so prominent due to very close spacing.

In order to study further the dependence of the athermal fading on the structural characteristics, the g fading factors of all samples were ploted together for the sake of comparison; these are presented in Fig. 5a. The data regarding the g-factors over all samples indicate that the corresponding values fall clearly within three distinctive groups, each one corresponding to the groups of sanidines, orthoclases and microclines. More specifically, for the case of sanidines, the values of the g fading factor yield smooth increase up to temperatures around 300 °C, and mild decrease over this temperature. For the case of orthoclases, a wide plateau is observed between 200 and 350 °C, followed by a smooth decline at higher temperatures. Finally for the case of microclines, smooth decrease is monitored within the temperature range between 200 and 450 °C. It is quite important to note that independent of the K-feldspar type, g fading factors decrease abruptly for temperatures over 450 °C. For a specific temperature, g factors of sanidines get highest values while the corresponding of microclines the lowest values. This latter feature stands in excellent agreement to Fig. 4.

Similarly, Fig. 5b presents the g_{50} factors of all samples. In this case, the corresponding data over all samples indicate that the values fall clearly in two groups, one corresponding to the group of sanidines solely, while the other group includes both orthoclases and microclines.

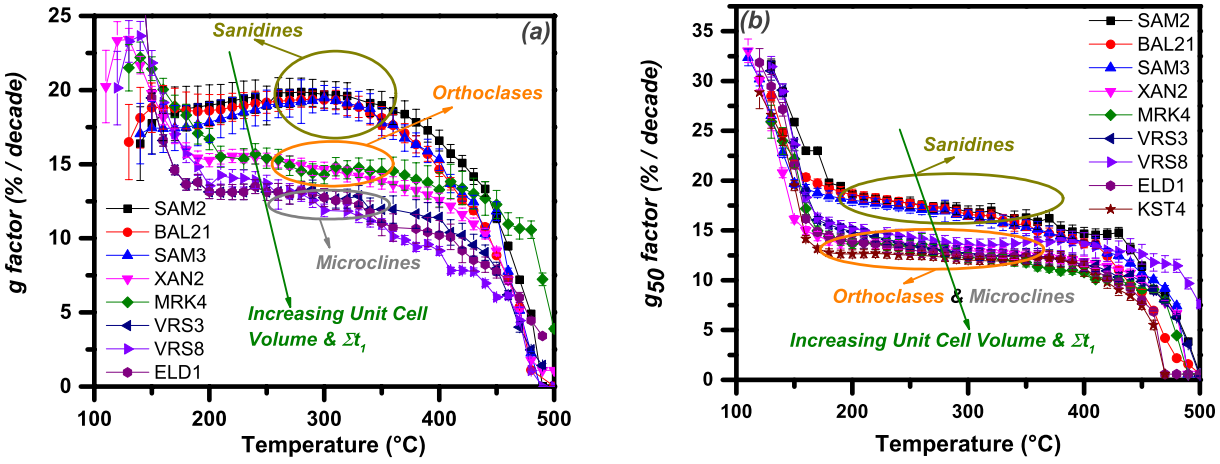

Fig. 5. Fading rate results on the K-feldspar samples of the present study consisting of the plots of both fading factors g (plot **a**) and g_{50} (plot **b**) within intervals of 10 °C versus the TL glow curve temperature.

For the former group, the values of g_{50} factors yield a smooth linear decrease for temperatures up to 400 °C, that becomes faster over 400 °C. In contrast, for either cases of microclines and orthoclases, the values of g_{50} factors form a wide plateau within the range 200 and 400 °C. In all cases, a steep decrease is monitored over 400 °C. Discrimination between orthoclases and microclines within the former group using only the g_{50} factor is not possible. This latter factor is calculated using Eq. (3) and via the dimensionless density of acceptors' parameter ρ'. Fig. 6 shows the behavior of this latter parameter ρ' versus the TL glow curve temperature for a selection of samples that include one microcline, one sanidine and one orthoclase. Only one example is presented for each group. As this figure strongly suggests, the dependence of the dimensionless density of acceptors is quite mild to both TL glow curve temperature as well as to the structural state characteristics of the K-feldspars. Similar results were also reported by Angeli et al. (2020), regarding the dependence of the values of parameter ρ'on the structural state characteristics of the K-feldspar samples. Thus the dependence of the g_{50} factor on characteristics such as the unit cell volume or the probability to occupy the T_1(o) and T_1(m) sites Σt_1, reflects the dependence of the parameter ρ' on such features.

The final result of the present study indicates that the ubiquitous athermal fading phenomenon is more intense in sanidines and less intense in microclines. This is not the first time that macroscopic experimental luminescence features are correlated to microscopic structural state characteristics of the K-feldspar samples (Biswas and Singhvi, 2013; Angeli et al., 2020 and references therein). In fact, as sanidines yield the lowest unit cell volume among all three groups, it is quite straightforward to consider that at the same time K-feldspars of this group indicate quite high values of charge density and consequently the highest values for the dimensionless parameter ρ'. The present manuscript indicates that AF in K-feldspar samples take advantage of the nearest pairs of donnor and acceptor charges. In microcline samples where the local dimensionless parameter ρ' is lower than in all other groups, AF is less intense.

Finally, it is important to note that in both cases of remnant TL after 30 days storage time (Fig. 4) as well as either g or g_{50} factors plotted versus temperature (Fig. 5) plateaus are formed within specific temperature regions and with varying temperature widths. Those plateaus, wherever available, indicate trapping states with similar athermal fading characteristics on the timescales considered. As each group of K-feldspars indicates individual AF features, a prevalent correction is not possible over all K-feldspars. Instead, such a correction might be possible for each group of K-feldspars independently.

5. Conclusions

- Fading rate was studied in two ways (a) by plotting the remnant TL after storage time of 1 month (namely the ratio $\frac{TL_{30\ days}}{TL_0}$) versus TL glow curve temperature and (b) by calculating both fading factors g and g_{50} (the latter describes the fading rate when the TL signal has been reduced to 50% of the prompt value measured after irradiation) within intervals of 10 °C within the entire TL glow curve and plotting them versus TL glow curve temperature.
- As the TL glow curves of K-feldspars are quite complex, calculation of the fading rate within intervals of 10 °C throughout the entire TL glow curve region over all potassium feldspar samples was helpful in identifying the temperature ranges at which the signal loss is seen simply due to either the lifetime of charge at room temperature or anomalous fading.
- The wide plateau of both g and g_{50} parameters suggests that anomalous fading is ubiquitous over the TL glow curve within 200–380 °C in all K-feldspar samples.
- The values of these aforementioned fading parameters are clearly correlated to the crystal structure of the K-feldspars.
- Among the three groups of K-feldspars, sanidines yield more intense athermal fading while microclines yield weak athermal fading.
- Discrimination among the three different groups could be achieved using the g fading factor but not the g_{50} factor.
- Due to mild dependence of either g and g_{50} factors on the TL glow curve temperature, the present study suggests the term "anomalous" instead of "athermal" fading.

Declaration of competing interest

The authors declare that they have no known competing financial interests or personal relationships that could have appeared to influence the work reported in this paper.

References

Aitken, M.J., 1985. Thermoluminescence Dating. Clarendon Press.

Angeli, V., Kitis, G., Pagonis, V., Polymeris, G.S., 2020. Sequential two-step optical stimulation in K-feldspars: correlation among the luminescence signals and implications for modeling parameters. J. Lumin. 226, 117425.

Auclair, M., Lamothe, M., Huot, S., 2003. Measurement of anomalous fading for feldspar IRSL using SAR. Radiat. Meas. 37 (4–5), 487–492.

Balian, H.G., Eddy, N.W., 1977. Figure of Merit (FOM): an improved criterion over the normalized chi-square test for assign the goodness-of-fit of gamma ray spectral peaks. Nucl. Instrum. Methods 145, 389–395.

Biswas, R.H., Singhvi, A.K., 2013. Anomalous fading and crystalline structure; studies on individual chondrules from the same parent body. Geochronometria 40 (4), 250–257.

Bøtter-Jensen, L., Bulur, E., Duller, G.A.T., Murray, A.S., 2000. Advances in luminescence instrument systems. Radiat. Meas. 32, 523–528.

Bowman, S.G.E., 1988. Nucl. Tracks Radiat. Meas. 14, 131.

Buylaert, J.P., Murray, A.S., Thomsen, K.J., Jain, M., 2009. Testing the potential of an elevated temperature IRSL signal from K-feldspar. Radiat. Meas. 44, 560–565, 2009.

Chen, R., McKeever, S.W.S., 1997. Theory of Thermoluminescence and Related Phenomena. World Scientific, Singapore.

Duller, G.A.T., 1997. Behavioural studies of stimulated luminescence from feldspars. Radiat. Meas. 27 (5–6), 663–694.

Huntley, D.J., Lamothe, M., 2001. Ubiquity of anomalous fading in K-feldspar and the measurement and correction for it in optical dating. Can. J. Earth Sci. 38, 1093–1106, 2001.

Jain, M., Guralnik, B., Andersen, M.T., 2012. Stimulated luminescence emission from localized recombination in randomly distributed defects. J. Phys. Condens. Matter 24, 385402.

Kitis, G., Kiyak, N.G., Polymeris, G.S., 2015. Temperature lags of luminescence measurements in a commercial luminescence reader. Nucl. Instrum. Methods Phys. Res. B 359, 60–63.

Kitis, Polymeris, G.S., Şahiner, E.V., Meriç, M., Pagonis, G., 2016. Influence of the infrared stimulation on the optically stimulated luminescence in four K-feldspar samples. J. Lumin. 176, 32–39.

Kroll, H., Ribbe, P.H., 1987. Determining (Al, Si) distribution and strain in alkali feldspars using lattice parameters and diffraction-peak positions: a review. Am. Mineral. 72, 491–506.

Pagonis, V., Brown, N.D., Peng, J., Kitis, G., Polymeris, G.S., 2021. On the deconvolution of promptly measured luminescence signals in feldspars. J. Lumin. 239, 118334.

Pagonis, V., Kitis, G., 2015. Mathematical aspects of ground state tunnelling models in luminescence materials. J. Lumin. 168, 137–144.

Pagonis, V., Kitis, G., Polymeris, G.S., 2020. Quantum tunneling processes in feldspars: using thermoluminescence signals in thermochronometry. Radiat. Meas. 134, 106325.

Pagonis, V., Phan, H., Ruth, D., Kitis, G., 2013. Further investigations of tunnelling recombination processes in random distributions of defects. Radiat. Meas. 58, 66–74.

Pagonis, V., Polymeris, G.S., Kitis, G., 2015. On the effect of optical and isothermal treatments on luminescence signals from feldspars. Radiat. Meas. 82, 93–101.

Polymeris, G.S., Sfampa, I.K., Niora, M., Stefanaki, E.C., Malletzidou, L., Giannoulatou, V., Pagonis, V., Kitis, G., 2018. Anomalous fading in TL, OSL and TA - OSL signals of Durango apatite for various grain size fractions; from micro to nano scale. J. Lumin. 195, 216–224, 2018.

Polymeris, G.S., Giannoulatou, V., Sfampa, I.K., Tsirliganis, N.C., Kitis, G., 2014. Search for stable energy levels in materials exhibiting strong anomalous fading: the case of apatites. J. Lumin. 153, 245–251.

Polymeris, G.S., Kitis, G., Pagonis, V., 2017. Thermoluminescence glow curves in preheated feldspar samples: an interpretation based on random defect distributions. Radiat. Meas. 97, 20–27.

Polymeris, G.S., Theodosoglou, E., Kitis, G., Tsirliganis, N.C., Koroneos, A., Paraskevopoulos, K.M., 2013. Preliminary results on structural state characterization of K-feldspars by using thermoluminescence. Mediterranean Archaeology and Archaeometry 13 (3), 155–161.

Polymeris, G.S., Şahiner, E.V., Meriç, M., Kitis, G., 2015. Thermal assistance in TA-OSL signals of feldspar and polymineral samples; comparison with the case of pure quartz. Radiat. Meas. 81, 270–274.

Polymeris, G.S., Tsirliganis, N.C., Loukou, Z., Kitis, G., 2006. A comparative study of anomalous fading effects of TL and OSL signals of Durango apatite. Phys. Status Solidi 203, 578–590.
Prasad, A.K., Poolton, N.R.J., Kook, M., Jain, M., 2017. Optical dating in a new light: a direct, non-destructive probe of trapped electrons. Sci. Rep. 7, 12097.
Ribbe, P.H. (Ed.), 1983, Feldspar Mineralogy, second ed., vol. 2. Mineralogical Society of America. Reviews in Mineralogy.
Sanderson, D.C.W., 1988. Fading of thermoluminescence in feldspars: characteristics and corrections. Nucl. Tracks Radiat. Meas. 14, 155–161.
Şahiner, E., Kitis, G., Pagonis, V., Meriç, M., Polymeris, G.S., 2017. Tunnelling recombination in conventional, post-infrared and post-infrared multi-elevated temperature IRSL signals in microcline K-feldspar. J. Lumin. 188, 514–523.
Sfampa, I.K., Polymeris, G.S., Pagonis, V., Kitis, G., 2019. Correlation between isothermal TL and IRSL in K-Feldspars of various types. Radiat. Phys. Chem. 165, 108386.
Sfampa, I.K., Polymeris, G.S., Pagonis, V., Theodosoglou, E., Tsirliganis, N.C., Kitis, G., 2015. Correlation of basic TL, OSL and IRSL properties of ten K-feldspar samples of various origins. Nucl. Instrum. Methods Phys. Res. B 359, 89–98.
Spooner, N.A., 1994. The anomalous fading of infrared-stimulated luminescence from feldspars. Radiat. Meas. 23 (2–3), 625–632.
Theodosoglou, E., Koroneos, A., Soldatos, T., Zorba, T., Paraskevopoulos, K.M., 2010. Comparative Fourier transform infrared and X-ray powder diffraction analysis of naturally occurred K-feldspars. In: Bulletin of the Geological Society of Greece, Proceedings of the 12th International Congress, Patras, pp. 2752–2761.
Thomsen, K.J., Murray, A.S., Jain, M., Bøtter-Jensen, L., 2008. Laboratory fading rates of various luminescence signals from feldspar-rich sediment extracts. Radiat. Meas. 43, 1474–1486.
Visocekas, R., Spooner, N.A., Zink, A., Blanc, P., 1994. Tunnel afterglow, fading and infrared emission in thermoluminescence of feldspars. Radiat. Meas. 23, 377–385.
Wintle, A.G., 1977. Detailed study of minerals exhibiting anomalous fading. J. Lumin. 15, 385–393.
Wintle, A.G., 1973. Anomalous fading of thermo-luminescence in mineral samples. Nature 245, 143–144.